Journal of Neuroscience Methods 146 (2005) 42–49

JOURNAL OF NEUROSCIENCE METHODS

www.elsevier.com/locate/jneumeth

An automated method to quantify and visualize colocalized fluorescent signals

Frédéric Jaskolski [a,*], Christophe Mulle [a], Olivier J. Manzoni [b]

[a] *Laboratoire "Physiologie Cellulaire de la Synapse", CNRS UMR 5091, Institut François Magendie, Université Bordeaux 2, Rue C. Saint-Saëns, 33077 Bordeaux Cedex, France*

[b] *Equipe INSERM Avenir, Plasticité Synaptique: Maturation and Addiction, Institut François Magendie, Université Bordeaux 2, Rue C. Saint-Saëns, 33077 Bordeaux Cedex, France*

Received 6 September 2004; received in revised form 14 December 2004; accepted 13 January 2005

Abstract

The most commonly used method to analyze colocalization of fluorescent signal in paired images is based on superimposition of images ("merging") and visual inspection. A method based on the comparison of the mean deviation of fluorescent signal intensity has recently been proposed to quantify colocalization within a user-defined area [Li Q, Lau A, Morris TJ, Guo L, Fordyce CB, Stanley EF. A syntaxin 1, Galpha(o), and N-type calcium channel complex at a presynaptic nerve terminal: analysis by quantitative immunocolocalization. J Neurosci 2004;24:4070–81]. Unfortunately, the latter quantification method does not provide a spatial representation of the correlation between the two fluorescent signals. Here we propose a new method that combines quantification and imaging of colocalization. We describe an algorithm based on edge detection and calculation of signal intensity deviation. The method is illustrated and validated on both simulated images and experimental data. This new and automated method calculates a correlation index (I_{corr}) and generates an image of the correlated signals from the two original images. In addition to help in comparing and quantifying colocalization between two fluorescent stainings, this method can be adapted to measure the distribution of ions, proteins, organelles and cells in a large array of techniques.

Keywords: Fluorescence; Image processing; Quantification; Correlation index; Colocalization

1. Introduction

Imaging of fluorescent signals is widely used in the field of life sciences to investigate the localization of ions, proteins, organelles and cells in a large array of techniques (e.g. immunocytochemistry, calcium imaging, immunohistochemistry, etc.). An often-asked question is whether two partners of interest are concentrated in the same domains, in other words whether they are colocalized or not. Signals are colocalized when they are observed in overlapping area and when their intensities vary in synchrony within a defined region. The most classical approach to determine the colocalization of fluorescent markers is based on the "dye-overlay method" (Li et al., 2004) (a.k.a. "merging"). This representation is based on the superimposition of fluorescent signals in two (or three) superimposed layers. It allows a binary estimation of whether the two fluorescent signals occur within the same or in different regions. The main advantage of "merging", beside its easiness, is that it preserves spatial information (contours and shape of the observed object). However "merging" is subject to the perception of the investigator and forbids any quantification. To quantify colocalization, the main approach is based on calculating the Pearson's correlation coefficient ("*r*", see Section 2) (Manders et al., 1992). This correlation index is useful for quantification but does not provide any information concerning the localization of both signals of interest. None of these methods combine the exploration of the two criteria that defines colocalization (i.e. overlapping and co-variation).

Li et al. (2004) have proposed a method named "intensity correlation analysis" that permits to quantify the colocaliza-

* Corresponding author. Tel.: +33 5 57 57 40 95; fax: +33 5 57 57 40 82.
E-mail address: fjaskol@pcs.u-bordeaux2.fr (F. Jaskolski).

0165-0270/$ – see front matter © 2005 Elsevier B.V. All rights reserved.
doi:10.1016/j.jneumeth.2005.01.012

tion of fluorescent signals. This method is derived from the measure of the deviation from the mean intensity for each pixel and for both signals in paired images, and yields a global correlation index for the paired images (like Pearson's correlation index "*r*"). The resulting single value can be used to quantify the correlation between the two original images but the spatial information (i.e. "the image") is still lost. Lately, another automated method to quantify colocalization has been proposed (Costes et al., 2004). This procedure is based on spatial statistics and enables quantification by thresholding the correlation of paired pixels.

Here, we propose a modification of the "intensity correlation analysis" method (Li et al., 2004). Our method permits the quantification of correlation while preserving the spatial information by evaluating correlation between pairs of individual pixels rather than between global images, and thus image the distribution of the degree of correlation for each pixel. This new method is set to define regions of interest (ROIs) in both paired images, create a single region to investigate the signal correlation, and calculate the correlation image, the overlapping fraction and an appropriate index of correlation. Correlation images provide a cross view of biological compartments and intensity variations revealing what was hidden in eye-based exploration. We tested our method on simulated images to explore a wide range of colocalized combinations and put it to the test on experimental data. This useful automated tool reduces as much as possible user-introduced biases and enables quantification and imaging of colocalization of two fluorescent signals.

2. Methods

2.1. Hippocampal cultures

Primary cultures of hippocampal neurons were obtained from 1-day-old pups of C57-BL/6 mice. Hippocampi were dissociated with papain followed by mechanical trituration and plated at 50,000 cells/cm^2 in MEM-EAGLE supplemented with 0.5% D-glucose, 0.1 mg/ml transferrin, 25 μg/ml insulin, 2 mM Glutamax (Life Technologies, France) and 5 μg/ml gentamycin; 2% B-27 (Sigma, MO, USA) and 1 μM cytosine arabinoside were added 3 days after plating.

2.2. Immunostaining

Cells were fixed in PFA (4%), and kept in PBS added with 0.3% BSA and 0.05% saponin during the steps that require membrane permeabilisation. Epitopes were detected using monoclonal anti-MAP2 antibody (Ab) (1:500, #HM-2, Sigma), polyclonal anti-MAP2 Ab (1:500, Peninsula Laboratories Europe), polyclonal anti-VGlut1 Ab (1:500) (Herzog et al., 2001), monoclonal anti-EEA1 Ab (1:500, BD Transduction Laboratories) and a monoclonal anti-GM1300 Ab (1:500, BD Transduction Laboratories) incubated for 1 h at RT. Secondary Ab are incubated for 1 h at 20 °C; Ab anti-rabbit Alexa 568 and 488 conjugated IgGs (#A-11011 and #A-11001, Molecular Probes, OR, USA), anti-mouse Alexa 568 and 488 conjugated IgGs (10 μg/ml, A-11008 and A-11004, Molecular Probes).

2.3. Image acquisition

Confocal images were acquired on a Leica TCS SP2 microscope. The exposure settings and gain of laser were kept the same for each condition. Ten fields were acquired by condition, a single focal plane by field (Airy 1).

2.4. Numeric treatment and algorithm generation

Image analysis, algorithm generation, statistical analysis and simulations were performed under MATLAB 6 software (MathWorks, Natick, MA, USA). The Matlab script is available at: http://www.synapse.u-bordeaux2.fr/pagesperso/jaskolski.htm.

2.5. Supplementary formulas

$$\text{Pearson's } r = \frac{\sum_{a,b}^{N}(a-\bar{a})(b-\bar{b})}{(N-1)(\sigma_a\sigma_b)}$$

δ_x is the variance for x.

3. Results

3.1. A method to select regions of interest based on edge detection by derivate approximation

Before evaluating colocalization of two stainings in paired images, it is necessary to determine the relevant "regions of interest" (ROIs) in both images in order to separate signal from background but also to determine a common region for both images in which putative signal fluctuations might be relevant. The most common approach is background exclusion based on a "manual intensity threshold" where the threshold can be subjectively estimated or calculated as a product of the mean background intensity (Jaskolski et al., 2004; Osten et al., 2000). This simple method is user-based and introduces obvious biases that may compromise the quantification of the resulting processed images. In order to reduce as much as possible such biases, we propose to use an approach based on the detection of signal edges by a "Sobel filter" (Gonzales and Woods, 2002). The method uses derivate approximation: inflections in the derivate occur when signal increases or decreases with steep slopes (Fig. 1A). Derivate approximation is performed using a two-dimensional convolution with "Sobel's kernels" (Fig. 2B) (Yoshigi et al., 2003). A threshold is then set in the distribution of local derivates to surround signal delimited by equal derivate values. Surrounded fields are filled to generate binary mask images. The ROI are obtained by multiplying the original image by the mask image. The

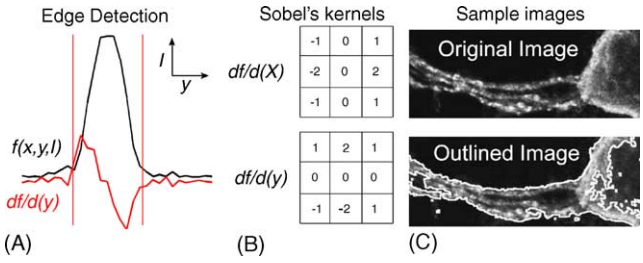

Fig. 1. Use of derivate approximation to define ROI. (A) Line-scan (*y*-axis) of 30 pixels among an image of fluorescence across a bright dot (black, obtain from image in C) and its derivate approximation (red). Red lines indicate how derivate approximation can be used to define the edges of the ROI. (B) "Sobel's kernels" successively used to calculate the derivate approximation. (C) Top image: crop of a stained neuron (immunostaining of surface expressed glutamate receptors); bottom panel: corresponding outlined image after edge detection with "Sobel's kernels".

threshold can be set as a product of the mean derivate in the non-relevant background regions. This method allows the determination of ROI with low user biases (Fig. 1C). ROIs are thus defined for both images. In the case of no colocalization, the ROI determined in the first image will be excluded from the ROI detected in the corresponding ("paired") image. To circumvent this problem we used a simple Boolean operation ("OR") in order to generate a single ROI that encompasses the relevant regions of both images. We can now define a single territory from a pair of images and use it to explore the correlation of both signals within the shared ROI. Finally, other methods like the "manual intensity threshold" can be used to define ROIs. The use of edge detection methods is not required to apply the correlation analysis method.

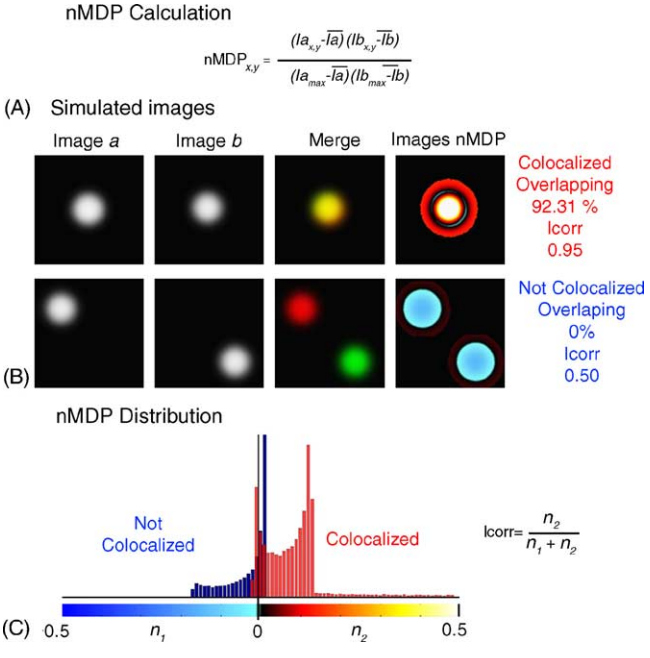

Fig. 2. Quantification and visualization of colocalized fluorescent signals. (A) Formula for nMDP calculation. "*x*" and "*y*" correspond to pixel coordinates, "I_a" is the intensity in image "a" for the given pixel, same for "I_b", barred "$\bar{I}_a$" and "$\bar{I}_b$" are mean intensity values across respective images (in the defined common ROI). Bracket expressions indexed "max" are the maximum mean deviations calculated in each image. (B) Generation of images nMDP starting with two sets of simulated images: a colocalized set (top row) and a not colocalized set (bottom row). (C) Distribution of nMDP values for the colocalized condition (red) and the not colocalized condition (blue) among the nMDP scale (−0.5 to 0.5). This scale is combined with an appropriate lookup table, from black to white in hot colours for positive nMDP values, in cold blue variations for negative nMDP values. The formula for I_{corr} calculation as the fraction of positive nMDP values (n_2) divided by the total calculated nMDP values ($n_1 + n_2$) is also given.

3.2. Quantification and visualization of colocalized fluorescent signals

Recently, Li et al. (2004) have proposed an alternative to the classical "dye-overlay" method, "intensity correlation analysis", which allows quantitative analysis of colocalized fluorescent signals. This method assumes that the intensity of two colocalized signals vary in synchrony over the selected image. It measures the mean intensity deviation in each pixel of the paired images and calculates the sum of the product of mean deviation over the selected ROI. The resulting single value is an index that reflects the global intensity of correlation between the two signals for the whole image. Other methods expressing the correlation in two images by a single value already exist (Manders et al., 1992) (e.g. Pearson's correlation index, see Section 2) and although they can provide a quantification of correlation they most notably share the disadvantage of losing spatial information. Ideally, one would like to implement a method that permits the quantification of correlation while preserving the spatial information over the paired images. Images are space functions of gray value intensity that we processed as matrix of entangled triplets: *x* and *y* positions and *I* as the gray value intensity (I_a, intensity in image a). We first calculated the mean intensity for both signals (a and b) over the ROI, and the mean deviation product for the two signals ($(I_a - \bar{I}_a)(I_b - \bar{I}_b)$) for each set of (*x*, *y*) coordinates. In order to compare series of images, we normalized these values by dividing with the product of maximum mean deviations and we obtained for each set of (*x*, *y*) coordinate the "normalized mean deviation product" ($nMDP = (I_a - \bar{I}_a)(I_b - \bar{I}_b)/(I_{a\,max} - \bar{I}_a)(I_{b\,max} - \bar{I}_b)$) (Fig. 2A). We then generated an image displaying the spatial distribution of calculated nMDP values (image nMDP, Fig. 2B) with an appropriate lookup table. The nMDP index varies from −1 to 1, where negative values represent non-correlated pixels while positive values indicate correlated pixels (Fig. 2C). The absolute value depends on the deviation to the mean of both I_a and I_b and thus quantifies the relationship between these values.

We first tested this method on artificial images generated to simulate either strong colocalization or no colocalization. As shown in Fig. 2, correlated pixels appear in "hot" colours ($nMDP > 0$) and non-correlated pixels in "cold" colours ($nMDP < 0$). The "black ring" in the colocalized image nMDP represents the region where the values tend toward the mean. It must be noted that pixels out of the ROI are

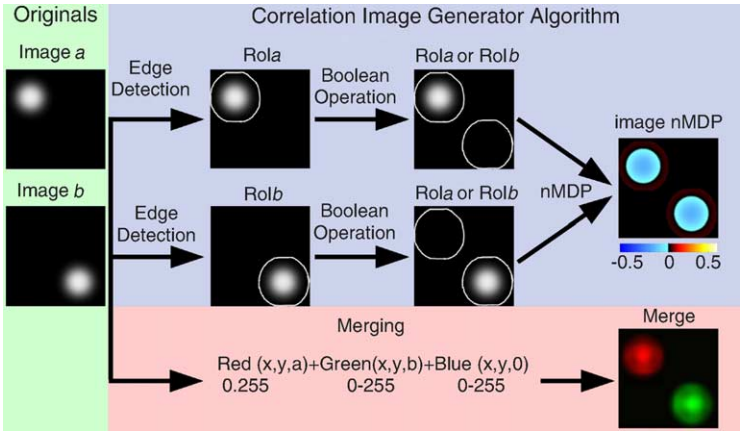

Fig. 3. Algorithm: schematic representation of the successive steps of the automated algorithm that generate image nMDP (blue box) from original images (green box). A third arm calculates the merged image (pink box).

represented in black in the image nMDP. Because a single index for each image pair is useful to sample and compare different conditions, we calculated the fraction of positively correlated pixels among the image nMDP. This value, I_{corr}, reflects the distribution of nMDP values (Fig. 2C).

3.3. Algorithm

In an image, gray values are discretely sampled from 0 to 255 for 8-bit indexed images and from 0 to 4095 in 12-bit indexed images. These variables cannot be used for derivate approximation or nMDP calculation (irrationals and negative numbers are generated). To overcome this problem we worked with matrices rather than images by converting 8-bit indexed images to three-dimensional matrices of double floating variables. We generated an algorithm using Matlab 6 software (MathWorks, Natick, MA, USA) that automates the successive steps required for the quantification of the colocalization of fluorescent signals in paired images using our nMDP algorithm (Fig. 3, blue box). The function first opens the images (Fig. 3, green box), asks for background selection then calculates the ROI in each image, applies the Boolean operator "OR" and calculates nMDP values. We have added in the algorithm an arm that calculates the merged image (Fig. 3, pink box). The function also displays two values, I_{corr} and the overlapping fraction of the two original ROIs (ROI_a and ROI_b). This procedure can be adapted to any software that allows matrix calculation and visualization. The Matlab script is available at: http://www.synapse.u-bordeaux2.fr/pagesperso/jaskolski.htm.

3.4. I_{corr} distribution

Next, we evaluated how the correlation index (I_{corr}) compares to the overlapping fraction and how it is distributed among all possible positions. Thus, we generated pairs of images (62×62 pixels) each containing a two dimension Gaussian signal of gray values (31×31 pixels). The Gaussian signal was randomly positioned in each image and the set of images was analyzed with the automated algorithm (without background selection). I_{corr} was plotted as a function of the overlapping fraction after 10,000 successive simulations (Fig. 4). The overlapping fraction corresponds to the number of pixels charred by the two first defined ROIs divided by the size in pixel of the complete ROI generated by the Boolean operator. Several possible distribution of both signals ranging from strong colocalization (Fig. 4A) to adjacent not overlapping (Fig. 4D) were explored. As expected, I_{corr} increased when the signals overlapped. Two regions (marked in gray) were not explored by the simulation: they correspond to 1/overlapping events that are not correlated (an impossible case) and 2/correlated images that only slightly overlap. This last case can be observed when the simulation is performed with two 2D Gaussians per image (data not show). It corresponds to cases where the calculated ROIs

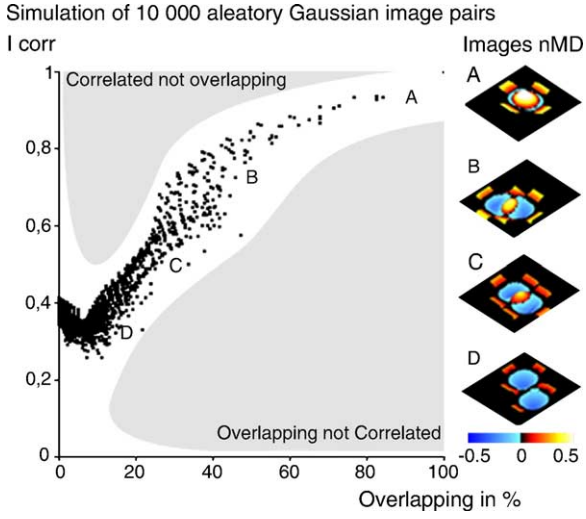

Fig. 4. Scatter plot, I_{corr} vs. the overlapping fraction calculated for 10,000 image pairs. Each image is composed of a 2D Gaussian curve randomly positioned. Left column displays four examples of images nMDP from strong colocalization (A) to close apposition (D) obtained during the simulation.

have different sizes so that the relative overlapping fraction is weak but signals are correlated within the whole explored region. An interesting observation is that the minimum I_{corr} is measured for 10% overlapping signals and that it slightly increases when the overlapping fraction tends to 0. In this configuration most pixels are under the mean in both images so that the resulting nMDP is positive and I_{corr} increases. In order to obtain an I_{corr} value around 0, the signals must be in opposite phases in the entire explored territory (we assume that this would be an extremely rare case).

Because experimental images are noisy, we next tested how different types of noise alter the nMDP correlation analysis. Two types of noise were added to the simulated images: a uniform Poisson noise (P_{noise}) corresponding to background and an intensity dependant noise (classically "light noise").

When P_{noise} is added to the two dimensions Gaussian signal, the correlation between I_{corr} and the overlapping fraction is maintained until the variance of P_{noise} reaches the order of magnitude of the signal variance (Fig. 5A). The limit observed when P_{noise} variance reaches signal variance is indeed due to the sensitivity of the Sobel's edge detection method to background. In this case, background can be mistaken for signal in each paired images (Fig. 5A, bottom image). This artefact limits the occurrence of large overlapping conditions while the I_{corr} index still reflects signal correlation (Fig. 5A, black scatter plot). This indicates that the nMDP method is only slightly affected by background noise.

Intensity dependent noise causes an increase in the signal variance (Fig. 5B). Such fluctuations of signal variance affect the nMDP calculation because they disrupt the point-to-point signal correlation that is measured by the mean deviation. However, "reasonable" intensity dependant noise (i.e. noise variance <200) does not affect the relation between I_{corr} and the overlapping fraction (Fig. 5B), strongly suggesting that the nMDP method is not critically affected by intensity dependent noise.

3.5. Experimental test

Finally, we tested our method on genuine images obtained from cultured neurons stained with two fluorescent markers. Cultured mouse hippocampal neurons (21 DIV) were fixed and immunostained with various antibodies in order to generate representative fluorescent signals. First, to obtain strong colocalization, neurons were labeled with two different antibodies directed against the same protein, the microtubule associated protein 2 (MAP2, a somato-dendritic marker), a rabbit polyclonal antibody and a mouse monoclonal antibody. Second, we labeled MAP2 together with the synaptic vesicular glutamate transporter 1 (VGluT1, a presynaptic marker of glutamatergic synapses) (Herzog et al., 2001). Third, we co-stained MAP2 and the early endosomal Rab5 effector protein (EEA1, known to be detectable in dendrites) (Wilson et al., 2000). Finally we co-stained MAP2 and GM130, a protein of the Golgi apparatus. For these four conditions we show the results of the "merging" method (Fig. 6A, upper line) and compare it to the corresponding nMDP image (Fig. 6A, bottom line). In each condition we acquired a set of 10 image pairs and calculated the mean overlapping fraction in % (Fig. 6B) and the mean I_{corr} (Fig. 6C). As expected, co-staining the same protein (MAP2) with two different antibodies results in strongly colocalized signals (Fig. 6A, first

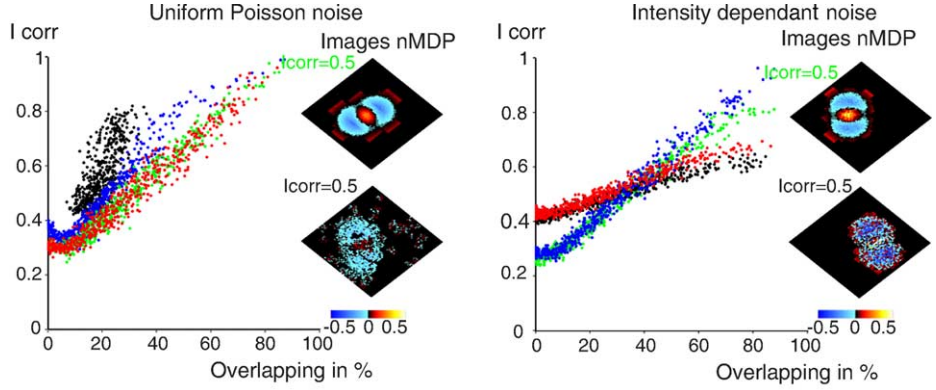

Fig. 5. Noisy simulated data. (A) Scatter plot, I_{corr} vs. the overlapping fraction calculated for 500 image pairs. Each image is composed of a 2D Gaussian curve randomly positioned and added with a uniform Poisson noise (P_{noise}) of defined variances. Blue, green, red, black, respectively, correspond to P_{noise} with variances 1, 10, 100 and 1000. On the right, two sample nMDP images obtained with P_{noise} variance 10 (top) and 1000 (bottom) for $I_{corr} = 0.5$. (B) Scatter plot, I_{corr} vs. the overlapping fraction calculated for 500 image pairs. Each image is composed of a 2D Gaussian curve randomly positioned and added with an intensity dependant noise ($N \times$ 2D Gaussian). N is normally randomized, mean = 0, blue, green, red, black, respectively, correspond to N variances 0.01, 0.1, 0.5 and 1, giving the indicated variances for $N \times$ 2D Gaussian. On the right, two sample nMDP images obtained with N variance 0.1 (top) and 1 (bottom) for $I_{corr} = 0.5$. Signal variances and $N \times$ 2D Gaussian variances are calculated approximations.

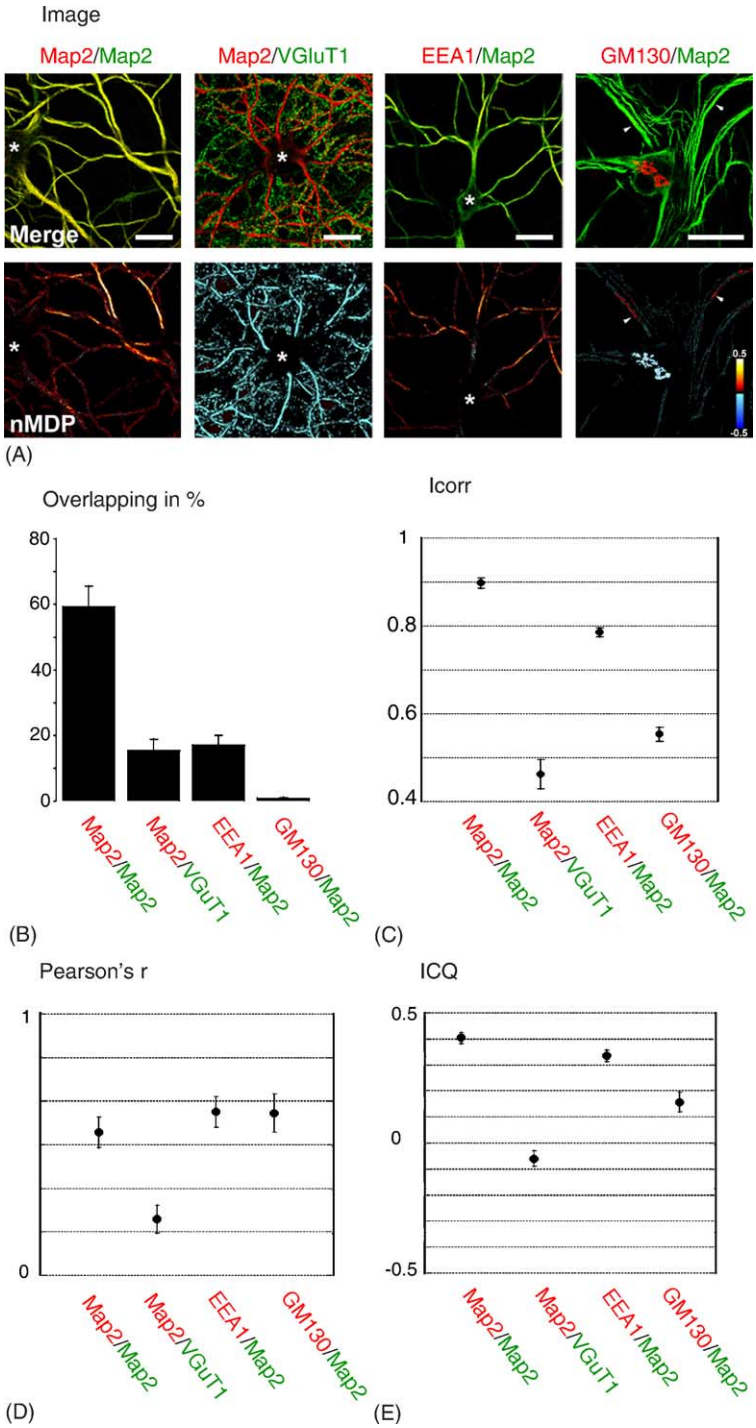

Fig. 6. Experimental data. (A) Merged images (top row) and images of nMDP (bottom row) obtained from four double staining conditions, MAP2/MAP2 (first column), MAP2/VGluT1 (second column), EEA1/MAP2 (third column) and GM130/MAP2 (fourth column). These four conditions explored different possibilities from strong colocalization (MAP2/MAP2, yellow in merged image and hot colours in image nMDP) to exclusion (MAP2/VGluT1, cold colours in image nMDP). White stars indicates the position of the soma, white arrow heads shows tubular structures positive for GM130 labeling, scale bar is 10 μm. (B) The mean overlapping fraction in % (±S.E.M.), (C) the mean I_{corr} (±S.E.M.), (D) the mean Pearson's r (±S.E.M.) and (E) the mean ICQ (±S.E.M.) calculated for each condition.

column): the mean overlapping fraction is small compared to the apparent colocalization (mean ± S.E.M., 59 ± 6%) while the mean I_{corr} index is close to 1 (0.89 ± 0.12). Double labeling for VGluT1 and MAP2 reveals that these two markers are not colocalized (cold colours in the image nMDP, Fig. 6A, second column), although the VGluT1 signal is found apposed to MAP2 labeling. The calculated mean overlapping fraction is not null (15 ± 4%) and the mean I_{corr} is slightly

under 0.5 (0.46 ± 0.03) suggesting that these markers are segregated. In fact, territories devoid of MAP2 labeling are filled by VGluT1 staining (and vice versa). In this particular case, intensity variations in coupled images are almost in opposed phases, when a pixel in the first image is above the mean intensity, the corresponding pixel in the paired image is under the mean intensity, yielding a negative value for the mean deviation product (and thus for the nMDP). The resulting nMDP distribution is shifted to the negative values and the I_{corr} index tends to be below 0.5. EEA1 and MAP2 overlaps to the same level as MAP2 and VGluT1 (EEA1/MAP2, $17 \pm 3\%$; MAP2/VGluT1, $15 \pm 4\%$), but EEA1 is also distributed along dendritic extensions and colocalizes with MAP2 (mean I_{corr}, 0.78 ± 0.01; hot colours in nMDP image, third column). As previously described, the Golgi apparatus is mainly concentrated around the nucleus in the neuronal soma (Dotti and Banker, 1991). Recently, GM130 positive tubular structures have been described in neurites (Horton and Ehlers, 2003). Imaging nMDP reveals the Golgi matrix in the soma (cold colour, Fig. 6A, last column) and some tubular structures in the dendrites (hot colour, white arrow heads, Fig. 5A). These tubular structures did not appear in the "merging" method because the GM130 signal is too weak compared to the MAP2 staining. The mean overlapping fraction is weak ($1.1 \pm 0.2\%$) because the ROI detected for GM130 is small compared to the ROI detected for MAP2, nonetheless the I_{corr} appropriately illustrates the relative non-colocalization of both markers (0.55 ± 0.01).

In order to compare the nMDP method to other methods, we have calculated the Pearson's r index and the ICQ (intensity correlation coefficient) described by Li et al. for our experimental conditions (Fig. 6D and E). The Pearson's r index (see Section 2) is a global index that efficiently identifies colocalized signals but does not differentiate between the MAP2/MAP2, the EEA1/MAP2 and the GM130/MAP2 conditions (Fig. 6D). To calculate the ICQ index, 0.5 is deducted to the fraction of pixels with positive mean deviation products divided by the total number of pixels explored ($ICQ = I_{corr} - 0.5$). Thus, the ICQ index detects the same variations as the I_{corr} index (Fig. 6D) but gives no indication on signal overlapping.

Across these examples it clearly appears that I_{corr} reflects with a high fidelity the relationship between two markers independently of their overlapping fraction. Moreover, using nMDP image allows the spatial exploration of this correlation and reveals what the "merging" method kept hidden.

4. Discussion

The labeling and visualization of two or more partners using imaging techniques is hampered by the intrinsic limit of optical imaging (i.e. the resolution of the image) but also by the image processing per se which in most cases heavily relies on user-based decisions and previous experiences and most often does not permit the detailed (i.e. pixel per pixel) quantification of the degree of colocalization. Here we propose a simple and fully automated method to quantify and visualize colocalization between two images.

Through the use of derivate approximation the method first defines an appropriate ROI without introducing user biases. This method is easy to implement (Yoshigi et al., 2003) but unfortunately remains rarely used. It must be noted that other convolution filters such as Canny's method, Prewitt's method or the Robert's method also permit the approximation of the local derivate in images (Gonzales and Woods, 2002). These various methods differ by their sensitivities and their orientations (derivate approximation is calculated among a direction, $df(x, y)/dx$, $df(x, y)/dy$ or $df(x, y)/d(x, y)$). They allow a good estimation of the local derivate and thus also permit reliable edge detection. Nevertheless, there is no requirement to use the derivate approximation to process the correlation calculation and any method generating ROIs could be successfully used. Second, the calculated nMDP reflects variations of signals around the mean. Other ways to correlate signals, such as deviation around the local mean (calculated in pixels around the pixel of interest) could alternatively be used. The main advantage of the nMDP is that the correlation is calculated for paired pixels sharing the same spatial coordinates. An important limit is that the mean calculation depends on the size of the ROI. For instance, if the two first defined ROI have extremely different sizes, the Boolean "OR" operation extends the field of mean calculation which may cause an underestimation of the mean intensity (and a corresponding overestimation of the mean deviation). In the nMDP algorithm these biases are moderated by the normalization but this potential caveat must be taken into account while analysing images nMDP. This limit can also be circumvented by using local mean deviation but this would increase difficulties in image processing.

The I_{corr} index represents the fraction of pixels with positive nMDP values. This property makes the I_{corr} index sensitive to the contribution of pixels with an nMDP value slightly greater than zero. This sensitivity might be considered for clear result reading.

Using experimental data and simulated images we show that: (1) the nMDP method is not critically affected by background noise and intensity dependent noise; (2) the simple calculation of a correlation index between two images is not sufficient to quantify colocalization. Here, we calculate the fraction of positive nMDP values among the total analyzed pixels (I_{corr}) and the overlapping fraction of stainings. Interestingly, the I_{corr} index is more discriminative than the Pearson's r index probably because the I_{corr} index is not dependant on signal variance. In conclusion, the nMDP method based on the parallel analysis of the overlapping fraction and the correlation index is a powerful tool to directly image colocalization.

Acknowledgements

The authors would like to thank Alexandre Thirouard for his technical help, Dr. Pascale Chavis and Dr. Martin Heine for critical reading of the manuscript and Pr. Marc Landry for helpful discussion.

References

Costes SV, Daelemans D, Cho EH, Dobbin Z, Pavlakis G, Lockett S. Automatic and quantitative measurement of protein–protein colocalization in live cells. Biophys J 2004;86:3993–4003.

Dotti CG, Banker G. Intracellular organization of hippocampal neurons during the development of neuronal polarity. J Cell Sci Suppl 1991;15:75–84.

Gonzales RC, Woods RE. Digital image processing. 2nd ed. Upper Saddle River: Prentice-Hall; 2002 p. 512–84.

Herzog E, Bellenchi GC, Gras C, Bernard V, Ravassard P, Bedet C, et al. The existence of a second vesicular glutamate transporter specifies subpopulations of glutamatergic neurons. J Neurosci 2001; 21:181.

Horton AC, Ehlers MD. Dual modes of endoplasmic reticulum-to-Golgi transport in dendrites revealed by live-cell imaging. J Neurosci 2003;23:6188–99.

Jaskolski F, Coussen F, Nagarajan N, Normand E, Rosenmund C, Mulle C. Subunit composition and alternative splicing regulate membrane delivery of kainate receptors. J Neurosci 2004;24:2506–15.

Li Q, Lau A, Morris TJ, Guo L, Fordyce CB, Stanley EF. A syntaxin 1, Galpha(o), and N-type calcium channel complex at a presynaptic nerve terminal: analysis by quantitative immunocolocalization. J Neurosci 2004;24:4070–81.

Manders EM, Stap J, Brakenhoff GJ, van Driel R, Aten JA. Dynamics of three-dimensional replication patterns during the S-phase, analysed by double labelling of DNA and confocal microscopy. J Cell Sci 1992;103(Pt 3):857–62.

Osten P, Khatri L, Perez JL, Kohr G, Giese G, Daly C, et al. Mutagenesis reveals a role for ABP/GRIP binding to GluR2 in synaptic surface accumulation of the AMPA receptor. Neuron 2000;27:313–25.

Wilson JM, de Hoop M, Zorzi N, Toh BH, Dotti CG, Parton RG. EEA1, a tethering protein of the early sorting endosome, shows a polarized distribution in hippocampal neurons, epithelial cells, and fibroblasts. Mol Biol Cell 2000;11:2657–71.

Yoshigi M, Clark EB, Yost HJ. Quantification of stretch-induced cytoskeletal remodeling in vascular endothelial cells by image processing. Cytometry 2003;55A:109–18.